Inorganic Chemistry

pubs.acs.org/IC

Featured Article

The One-Electron Reduced Active-Site FeFe-Cofactor of Fe-Nitrogenase Contains a Hydride Bound to a Formally Oxidized Metal-Ion Core

Dmitriy A. Lukoyanov, Derek F. Harris, Zhi-Yong Yang, Ana Pérez-González, Dennis R. Dean,* Lance C. Seefeldt,* and Brian M. Hoffman*

Cite This: *Inorg. Chem.* 2022, 61, 5459−5464

Read Online

ACCESS | Metrics & More | Article Recommendations | Supporting Information

ABSTRACT: The nitrogenase active-site cofactor must accumulate $4e^-/4H^+$ ($E_4(4H)$ state) before N_2 can bind and be reduced. Earlier studies demonstrated that this $E_4(4H)$ state stores the reducing-equivalents as two hydrides, with the cofactor metal-ion core formally at its resting-state redox level. This led to the understanding that N_2 binding is mechanistically coupled to reductive-elimination of the two hydrides that produce H_2. The state having acquired $2e^-/2H^+$ ($E_2(2H)$) correspondingly contains one hydride with a resting-state core redox level. How the cofactor accommodates addition of the first e^-/H^+ ($E_1(H)$ state) is unknown. The Fe-nitrogenase FeFe-cofactor was used to address this question because it is EPR-active in the $E_1(H)$ state, unlike the FeMo-cofactor of Mo-nitrogenase, thus allowing characterization by EPR spectroscopy. The freeze-trapped $E_1(H)$ state of Fe-nitrogenase shows an $S = 1/2$ EPR spectrum with $\mathbf{g} = [1.965, 1.928, 1.779]$. This state is photoactive, and under 12 K cryogenic *intracavity*, 450 nm photolysis converts to a new and likewise photoactive $S = 1/2$ state (denoted $E_1(H)^*$) with $\mathbf{g} = [2.009, 1.950, 1.860]$, which results in a photostationary state, with $E_1(H)^*$ relaxing to $E_1(H)$ at temperatures above 145 K. An H/D kinetic isotope effect of 2.4 accompanies the 12 K $E_1(H)/E_1(H)^*$ photointerconversion. These observations indicate that the addition of the first e^-/H^+ to the FeFe-cofactor of Fe-nitrogenase produces an Fe-bound hydride, not a sulfur-bound proton. As a result, the cluster metal-ion core is *formally* one-electron oxidized relative to the resting state. It is proposed that this behavior applies to all three nitrogenase isozymes.

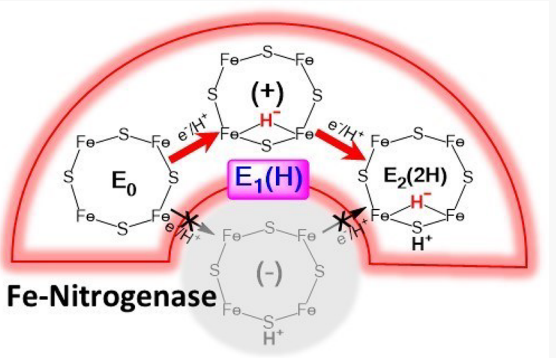

INTRODUCTION

The three nitrogenase isozymes (Mo-, V-, Fe-) reduce dinitrogen to two ammonia molecules in a multistep reaction involving two component proteins, an electron-delivery protein (Fe-Protein) and the N_2-reducing component, denoted MoFe-, VFe-, and FeFe-proteins, whose resting states contain the multimetallic (Fe_7M; M = Mo, V, or Fe) active site, called FeMo-, FeV-, and FeFe-cofactors, respectively.[1,2] The intermediates in the multistep catalytic cycle are labeled E_n, $n = 0$−8 for the number of e^-/H^+ additions, with bound substrate moieties (when known) indicated in parentheses (Scheme 1).[1] It has been shown that, despite significant differences in efficacy of the reduction of protons to H_2 and of N_2 to NH_3, the three isozymes follow the same reductive elimination step in the mechanism for N_2 binding/reduction.[3−8] From studies on the Mo-nitrogenase, it has been shown that binding of the N_2 substrate must be preceded by the accumulation of four electrons and protons by FeMo-cofactor to form the activated state $E_4(4H)$. In this state, the four electrons are associated with two hydrides bridging irons of the cofactor, two protons likely residing on the sulfurs, and a formal charge on the metal-ion core equal to that of the resting state (E_0).[9] N_2 binding to

Scheme 1. Simplified Lowe-Thorneley Scheme for the Nitrogen Fixation Catalytic Cycle of the Three Nitrogenase Isozymes[a]

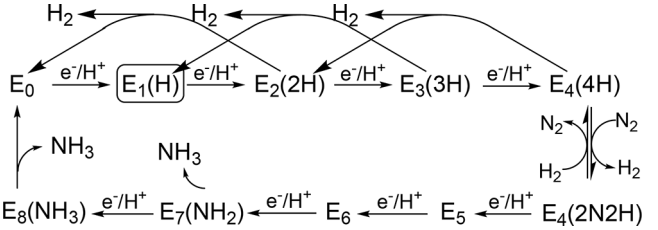

[a]The focus of this report is the first reduced state, $E_1(H)$, which is boxed.

Received: January 18, 2022
Published: March 31, 2022

the iron core of FeMo-cofactor is mechanistically coupled to the reductive elimination of two hydrides, the result being the loss of H_2 and formation of the first intermediate of N_2 reduction, E_4(2N2H), which contains reduced N_2 at the redox level of diazene.

It has been proposed that FeMo-cofactor utilizes only one redox couple (two formal redox states) across the eight electron/proton reduced states of the catalytic cycle.[8] Trapping and characterization of EPR-active catalytic intermediates shows that the metal core in E_n states, n = even, is in the same formal redox state as the E_0 state. This leaves a "binary" choice for the behavior of the n = odd intermediates. Focusing on the first step of e^-/H^+ accumulation[10] in the catalytic cycle (Scheme 1), there are two options for how the FeMo-cofactor stores the first e^-/H^+ on the way to the active state E_4(4H) (Scheme 2). It might be that the EPR-silent redox E_1(H) state

Scheme 2. Cartoon of Fe 2,3,6,7 Face of FeMo-Cofactor during Accumulation of First 2[e^-/H^+], with Alternative Possibilities for the Behavior of E_1(H)

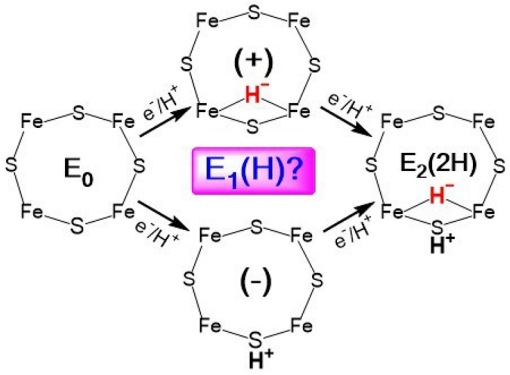

of FeMo-cofactor is formed by one-electron reduction of the metal core accompanied by protonation of a sulfide. Alternatively, addition of the first e^-/H^+ might form a bound hydride, with the hydride's second electron being donated by FeMo-cofactor, in which case the metal core thereby becomes formally oxidized by one electron. In either case, addition of the second e^-/H^+ forms E_2(2H), which photolysis experiments have shown containing a single hydride, with a proton bound to a sulfur of FeMo-cofactor and the metal core formally at the redox level of the E_0 state.[11]

EPR/ENDOR spectroscopy coupled with *intra*cavity photolysis has proven to be an effective test for hydride bound to Fe in EPR-active states of FeMo-cofactor of Mo-nitrogenase, E_n, n = even,[5,11,12] but the EPR-silent E_1(H) state of FeMo-cofactor prevents such a study. We therefore use the Fe-only isozyme to characterize E_1(H). In the resting (dithionite-reduced) state, FeMo-cofactor is EPR active (S = 3/2), but FeFe-cofactor is diamagnetic (S = 0).[13] Thus, while the FeMo-cofactor of E_1(H) is EPR-silent, the FeFe-cofactor of this state is EPR active.[13] If the E_1(H) were formed by reduction of the FeFe-cofactor core with proton binding to sulfide, then EPR spectroscopy would show it to be insensitive to photolysis. Alternatively, if this state contains a bound hydride, with a corresponding formal oxidation of the core, EPR spectroscopy would reveal the hydride by its photolability, Scheme 2. The study of the EPR-active E_1(H) state of FeFe-cofactor with photolysis/EPR reported here distinguishes between these two possible alternatives for the Fe-nitrogenase E_1(H) state.

MATERIALS AND METHODS

Reagents and General Procedures. All reagents were obtained from Sigma-Aldrich (St. Louis, MO), Fisher Scientific (Fair Lawn, NJ), or Bio-Rad (Hercules, CA) unless specified otherwise and used without further purification. Argon and dinitrogen gases were purchased from Air Liquide America Specialty Gases LLC (Plumsteadville, PA). Manipulation of proteins and buffers was done anaerobically in septum-sealed serum vials and flasks using a vacuum Schlenk line under an argon atmosphere. Gas transfers were made using gastight syringes.

Bacterial Strain Growth, Protein Purification, and Sample Preparation. Fe-nitrogenase component proteins, Fe protein (AnfH) and FeFe protein (AnfDGK), were expressed in *Azotobacter vinelandii* strain DJ2241 under previously described conditions.[14] Apo-FeFe protein (AnfDK) was expressed in *Azotobacter vinelandii* strain DJ2245 and purified as previously described.[15] FeFe protein ($anfD^{strep}$) and Fe protein were purified by previously described methods.[14] For resting state samples, FeFe protein was brought to a final concentration of 50 μM with a buffer of 50 mM Tris-HCl, 150 mM NaCl pH 7.0, and 10 mM sodium dithionite. A total of 300 μL of the sample was then added to a 4 mm quartz EPR tube and frozen in a pentane slurry. For turnover samples, FeFe protein and Fe protein were mixed at final concentrations of 50 μM and 5 μM in a previously described turnover buffer[16] and allowed to turnover at room temperature for 5 min. A total of 300 μL of the sample was then added to a 4 mm quartz EPR tube and frozen in a pentane slurry. For D_2O samples, proteins were exchanged into a D_2O buffer of 50 mM Tris-DCl, 150 mM NaCl pH 7.0, and 2 mM sodium dithionite before preparation of the sample.

EPR Spectroscopy and Photolysis. EPR spectra were recorded on an X-band Bruker ESP 300 spectrometer equipped with an Oxford Instruments ESR 900 continuous liquid helium flow cryostat. Spectra were simulated with EasySpin software.[17] *In situ* irradiation of samples at cryogenic temperature was performed through a waveguide beyond cutoff (microwave nontransmitting) attached to the cavity front face, with use of a Thorlabs Inc. (Newton, NJ) PL450B, 450 nm Osram Laser Diode with power adjusted to 45 mW.[12] Data points for the time course of photoinduced conversion of E_1(H) and E_1(H)* states were obtained as amplitudes of the well resolved g_3 feature of their spectra after correction for background associated with the EPR spectrum of the photostable inactive oxidized P-cluster.

RESULTS

EPR Spectroscopy. The FeFe-protein is EPR-silent in the dithionite-reduced E_0 resting state and presumed to be diamagnetic, S = 0.[13,18,19] Thus, EPR-active intermediates trapped during turnover in the absence of N_2 must correspond to E_n(nH), n = 1 or 3. Previous studies of the enzyme isolated from *R. capsulatus* have identified a low-spin (S = 1/2) EPR-active state with **g**-tensor components, **g** = [1.96, 1.92, 1.77],[13] that accumulates and is trapped during turnover with low ratios of Fe protein to FeFe protein (low electron-flux turnover) and thus is assignable to E_1(H), as accumulation of E_3(3H) would require high electron flux during turnover.

The FeFe protein isolated from *A. vinelandii* exhibits an axial signal with $g_{\|}$ = 2.06 and $g_{\perp}$ = 1.93 (Figures 1, S1) that was previously reported by Hales and co-workers[18,19] for this FeFe protein and assigned to its oxidized P cluster. We have confirmed the assignment to P cluster by its observation from apo-FeFe protein deficient in FeFe-cofactor (Figure S2).[15] A similar signal was also reported for resting state of V-nitrogenase. However, the assignment of that signal to the oxidized P cluster and the catalytic relevance of the species displaying that signal have been under debate.[10,20,21] Most

https://doi.org/10.1021/acs.inorgchem.2c00180
Inorg. Chem. 2022, 61, 5459−5464

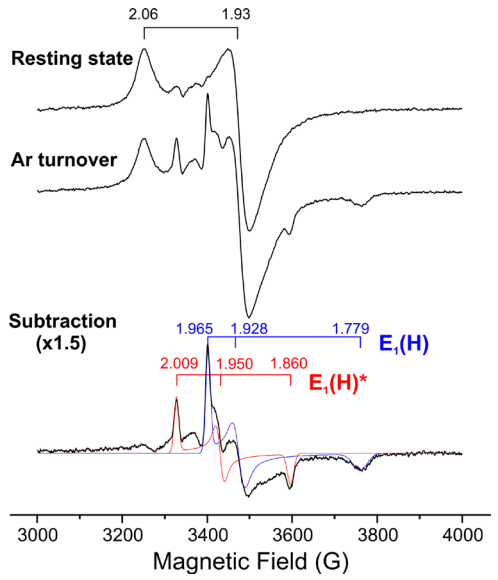

Figure 1. EPR spectra of Fe-nitrogenase. (Top) Enzyme in isolated resting state. (Middle) Enzyme trapped during Ar turnover. (Bottom) Subtraction of resting-state EPR signal from turnover signal with decomposition into $E_1(H)$ and $E_1(H)^*$ components (×1.5). Thin red and blue lines are EasySpin simulations. Conditions: T = 12 K; microwave frequency, 9.36 GHz; microwave power, 1 mW; modulation amplitude, 6 G; time constant, 160 ms; field sweep, 10 G/s.

recently, this state was proposed to be either a P-cluster precursor or catalytically inactive form of V-nitrogenase P cluster, and this needs to be further resolved.[18,22,16]

Two S = 1/2 state signals from functional *A. vinelandii* Fe-nitrogenase appear in varying ratios in EPR spectra of samples trapped during low-flux turnover under Ar, Figure 1. The first signal has **g** tensor [1.965, 1.928, 1.779]. It is equivalent to that previously reported for the turnover-trapped intermediate of *R. capsulatus* Fe-nitrogenase[13] and thus is assigned to the $E_1(H)$ intermediate. This state accumulates during turnover at ambient temperature. The second S = 1/2 signal, whose intensity relative to that of $E_1(H)$ varies from sample to sample, originates from a previously unreported intermediate state denoted here as $E_1(H)^*$, which has a rhombic **g** tensor, **g** = [2.009, 1.950, 1.860], whose g_1 and g_3 features could be easily resolved in the spectra. For a given sample of FeFe protein, the axial signal of the P-cluster is invariant under all conditions: unchanged during turnover, by intracavity photolysis, and by cryoannealing after photolysis (see below). Thus, as illustrated in Figure 1, the P-cluster signal can be completely subtracted with the same reference spectrum after any of those treatments, thereby clearly revealing the $E_1(H)$ and $E_1(H)^*$ signals for quantitation and simulation with EasySpin software.

PHOTOLYSIS

During intracavity irradiation at cryogenic temperatures with a 450 nm diode laser, the EPR signal from the $E_1(H)$ state of the FeFe-cofactor decreases in parallel with the increase of the spin S = 1/2 state $E_1(H)^*$ (Figures 2, S3). Simulations of the EPR spectra collected before and after irradiation, and of the difference between those spectra, show that there are no other significant photoinduced changes (see Figures 2, S3). The photolability of the $E_1(H)$ state is an indication that it is a hydride bound state, in agreement with the photolability of inorganic hydride complexes,[23,24] the two [Fe−H−Fe] bridging hydrides of the $E_4(4H)$ state of FeMo-cofactor,[12,25,26] and those of the single hydride of FeMo-cofactor of both hydride isomers of the $E_2(2H)$ state (EPR signals denoted 1b and 1c).[11] Photoinduced conversions of the hydride-bound states of FeMo-cofactor were completely reversed by cryoannealing the frozen solids, with a significant kinetic isotope effect (KIE) for both photolysis and cryoannealing as measured by comparing results for samples prepared in H_2O and D_2O buffers.

Whereas the result of photoinduced $E_1(H)/E_1(H)^*$ conversion is stable at 77 K, cryoannealing of the photolyzed FeFe-protein at 145 K for just 1 min gave an interesting and instructive result, Figure S3. First, both photoinduced $E_1(H)^*$

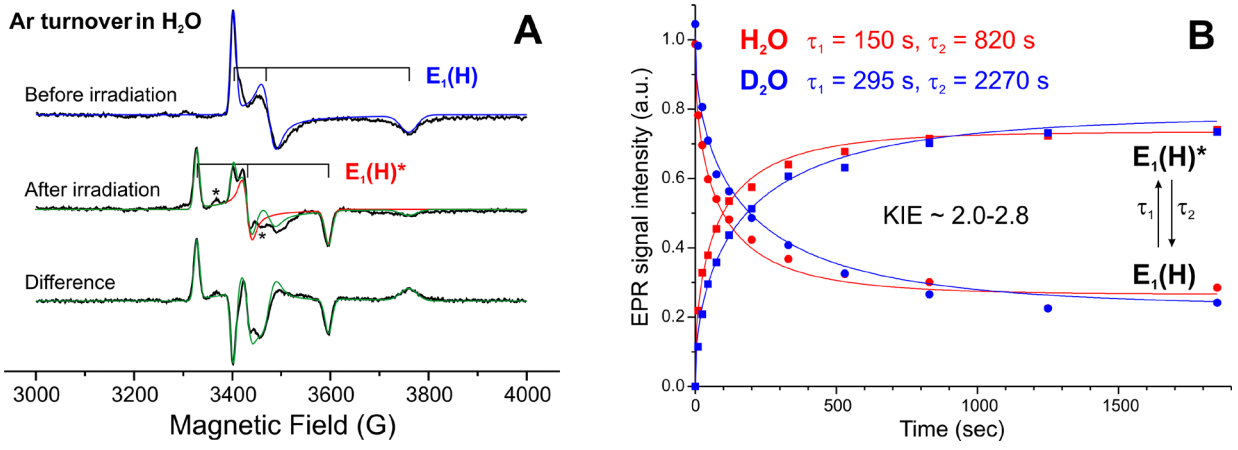

Figure 2. Photoinduced conversion of $E_1(H)$ and $E_1(H)^*$ states during irradiation of Fe-nitrogenase turnover samples with 45 mW of 450 nm laser diode at 12 K. (A) EPR spectra of turnover sample before and after irradiation, and their difference. Both spectra are shown after subtraction of the resting-state EPR signal. Blue/red lines are simulations of $E_1(H)/E_1(H)^*$ states; green lines are sums of these simulations. The asterisks (*) indicate features from a minor unassigned product of irradiation (see Figure S3 for more details). Conditions: as in Figure 1. (B) The time-courses of $E_1(H)$ (circles) and $E_1(H)^*$ (squares) populations observed during irradiation of samples prepared in H_2O (red) and D_2O (blue) and fitted with a kinetic scheme involving interconversion of the states, using stretched exponential functions $\exp(-(t/\tau_i)^m)$ with $m \sim 0.6$; the two rate parameters describing each trace, τ_1 and τ_2, as shown in the figure, are listed there.

https://doi.org/10.1021/acs.inorgchem.2c00180
Inorg. Chem. 2022, 61, 5459−5464

and the $E_1(H)^*$ present in the sample prepared by freeze-quenching during turnover relaxed to $E_1(H)$ during this brief cryoannealing (Figure S3). This suggests that $E_1(H)^*$ is not formed during turnover and trapped by freezing at all but rather is photoinduced by room light hitting the frozen sample during handling and storage in liquid nitrogen. To test this, the cryoannealed sample, which had no $E_1(H)^*$ signal, was first stored at 77 K in a transparent finger Dewar for 30 min in the dark, with no change in EPR response, and then for the same time under room light. This latter treatment produced the $E_1(H)^*$ signal, which thus confirmed a rather high photosensitivity of $E_1(H)$ (Figure S4). This finding guided the protocol for obtaining the time course of photoinduced loss of $E_1(H)$ in H_2O and D_2O turnover samples: first samples were annealed at 185 K for 2 min in the dark to erase the $E_1(H)^*$ state and to maximize the $E_1(H)$ state (Figure 2A) and then transferred in the dark to the EPR cavity. After each step of photolysis, the cavity window was covered to avoid room-light irradiation of the sample during EPR measurement.

Progress curves for the photoinduced loss of $E_1(H)$ and appearance of $E_1(H)^*$ states in both H_2O and D_2O turnover samples were generated from the time-dependent amplitudes of the corresponding EPR signals. As shown in Figure 2B, at every time during photolysis, the increase in the $E_1(H)^*$ signal corresponds to the loss of $E_1(H)$ as normalized to a constant value for the sum of concentrations, $(E_1(H) + E_1(H)^*)$. This indicates that photoexcitation of $E_1(H)$ in the frozen state causes the $E_1(H) \rightarrow E_1(H)^*$ conversion as a single kinetic step without buildup of an intermediate state.

Figure 2B further shows that photolysis does not go to completion but rather approaches steady-state populations with $E_1(H)$ and $E_1(H)^*$ in a roughly 1:3 ratio. This indicates that $E_1(H)^*$ also is photolabile, with a photostationary steady state achieved by a process of mutual conversion of the two photolabile states. It in turn implies that $E_1(H)^*$ likewise contains a metal hydride and is an isomer of the hydride bound to the cofactor of $E_1(H)$. The unequal populations in the steady state imply that the quantum yield for isomerization is about 3-fold greater for $E_1(H)$ than $E_1(H)^*$.

The photolysis time courses of $E_1(H)$ and $E_1(H)^*$ obtained for H_2O and D_2O turnover samples were fitted to the proposed process of state interconversion, using stretched-exponential functions, $\exp(-(t/\tau_i)^m)$, with time constants τ_1 and τ_2 for the $E_1(H) \rightarrow E_1(H)^*$ and $E_1(H)^* \rightarrow E_1(H)$ conversion, respectively, as shown in the Figure 2B. Stretched-exponential functions represent the distribution of apparent photolysis yields caused by light scattering in the nontransparent frozen samples (Figure 2B).[26] This functional form is equivalent to a time-dependent rate of photolysis,[27] and use of the previously described solution of the resulting differential equations[28] for the interconversion yields ratios of the respective time constants for reaction in H_2O and D_2O that correspond to a KIE ~ 2.4 for photolysis of turnover samples, which is close to the KIE of photoinduced conversion of the single-hydride state $E_2(2H)$ of FeMo-cofactor.[3,11] The presence of a KIE supports the conclusion that $E_1(H)$ and $E_1(H)^*$ are indeed hydride-bound states and that the rate-limiting step for interconversion is photoisomerization of the Fe-bound hydride.

DISCUSSION

We earlier proposed that throughout the $8[e^-/H^+]$ nitrogenase catalytic cycle (Scheme 1) the catalytic cofactor toggles between only two formal redox states.[8] Numerous EPR-active, MoFe protein E_n, n = even, intermediates have been trapped, and in each case the FeMo-cofactor can be described as formally exhibiting the E_0 redox level, with the additional electrons associated with bound substrate-derived ligand(s). In particular, this has been explicitly demonstrated for $E_2(2H)$[11] and $E_4(4H)$,[6,7,9,29] which we have shown, respectively, to contain one and two Fe-bound hydrides and an E_0-level metal-ion core. Given our finding that hydride chemistry is central to nitrogen fixation by nitrogenase, we further recognized that an n = odd state is formed by the addition of one e^-/H^+ to the preceding n = even state, and proposed that the proton "recruits" an electron from the core and forms an Fe-bound hydride, thus producing a formally oxidized core as the second redox level that is accessed catalytically.[3,11,8]

The central finding of the present study is that the $E_1(H)$ isomeric states indeed contain a FeFe-cofactor with a hydride bound to iron, which then leads by definition to a formal redox level of the metal-ion core in agreement with our earlier proposal: the addition of one e^-/H^+ to FeFe-cofactor in the E_0 state produces an Fe-bound hydride, thus formally *oxidizing* the metal core, the upper pathway of the redox reaction scheme presented in Scheme 2. The relationship of this formulation to our recent X-ray absorption/Mossbauer studies[10] and an earlier EXAFS study[30] is addressed immediately below. Considering the finding that all three nitrogenases exhibit the same reductive-elimination mechanism of N_2 activation at the $E_4(2N2H)$ state and share analogous cofactor structures, it seems reasonable to assign the $E_1(H)$ state in each of the three isozyme cofactors (FeMo-cofactor, FeV-cofactor, and FeFe-cofactor; denoted here as $E_1(H)$) as having an Fe-bound hydride and formally one-electron oxidized metal core.

Of course, we recognize the limitations to the formal description of redox level. The electrons associated with the hydride are covalently shared with the anchoring Fe ions, and K-edge XAS of FeMo-cofactor shows changes associated with reduction at Fe (not at Mo) upon the $E_0 \rightarrow E_1(H)$ conversion,[10] reversing the implication of cofactor oxidation from an earlier EXAFS study.[1,30] The key finding of the present study is that $E_1(H)$ and $E_1(H)^*$ both contain an Fe-bound hydride, rather than a proton bound to sulfide. The formal assignment of a redox level, that the cofactor is oxidized relative to that of E_0, then follows directly. The generality of this behavior can be tested by carrying out analogous experiments on $E_1(H)$ of the VFe-protein, which also is EPR-active.

There are several noteworthy comparisons to be made between photolysis of the Fe-nitrogenase $E_1(H)$ state and the photoinduced 1b → 1c* conversion of Mo-nitrogenase $E_2(2H)$/1b state, while recognizing that although both $E_1(H)$ and $E_2(2H)$ intermediates contain a bound hydride, in 1b the FeMo-cofactor core is at the formal resting-state redox level, whereas in $E_1(H)$, FeFe-cofactor has an oxidized core. First, the $E_1(H)$ state of FeFe-cofactor is more photosensitive than $E_2(2H)$ of FeMo-cofactor. The data of Figure 2B required about half the power of the 450 nm diode laser relative to that used for measuring the irradiation kinetics of the FeMo-cofactor $E_2(2H)$ state, with the decrease required to slow the reaction enough for analysis of the kinetics time course. Second, a steady state $E_1(H)^*/E_1(H)$ population ratio was established during FeFe-cofactor photolysis after ~10 min of irradiation of an H_2O sample, while for the FeMo-cofactor, 1b/1c* conversion of $E_2(2H)$ proceeded without reaching a

https://doi.org/10.1021/acs.inorgchem.2c00180
Inorg. Chem. 2022, 61, 5459−5464

steady state after 20 min of more intense irradiation.[11] In short, both $E_1(H)$ and $E_1(H)^*$ hydrides are highly photoreactive, whereas the $E_2(2H)/1c^*$ hydride is much less photosensitive than that of $E_2(2H)/1b$. As the third difference between the photolysis of $E_2(2H)$ of FeMo-cofactor and $E_1(H)$ of FeFe-cofactor, the photoinduced conversion of $E_1(H)$ into $E_1(H)^*$ can be completely reversed after just 1 min at 145 K (Figure S3), whereas relaxation of the photogenerated FeMo-cofactor $E_2(2H)/1c^*$ conformer occurs only slowly during annealing at this temperature, which allowed the kinetics of this process to be studied.

Despite these differences, as shown in Scheme 3, it seems likely that the hydride of $E_1(H)$ adopts one of the two bridging

Scheme 3. Possible Structures for the Interconverting $E_1(H)/E_1(H)^*$ Conformers

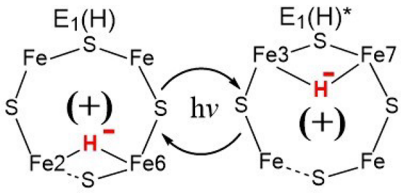

hydrides of the $E_4(4H)$ FeMo-cofactor state, whereas the hydride of $E_1(H)^*$ is the second bridging hydride of $E_4(4H)$.

SUMMARY

We have shown that the Fe-nitrogenase $E_1(H)$ state, in which the FeFe-cofactor has gained $1e^-/H^+$ relative to the E_0 state during turnover, exhibits properties consistent with a single hydride bound to a formally oxidized FeFe-cofactor, Scheme 2, upper. The light-induced changes in the EPR spectrum of the trapped species indicate there are two conformers of the hydride-bound $E_1(H)$ state, both photolabile but having different sensitivities to irradiation and stabilities to cryoannealing. The less photosensitive $E_1(H)^*$ conformer cannot accumulate during turnover as it is unstable at $T \geq 145$ K and relaxes to the $E_1(H)$ conformer, which is stable even during ambient-temperature turnover as expected for an intermediate in the catalytic reduction of N_2. However, at cryogenic temperatures, Fe-nitrogenase can be photoconverted into a photostationary state with both $E_1(H)$ and $E_1(H)^*$ present. Given the similarities in the catalytic cofactors and the common mechanism of nitrogen fixation (Scheme 1) for the three nitrogenase isozymes, it seems reasonable to propose that delivery of a single e^-/H^+ to the cofactor of each would create a hydride bound to a core that is therefore formally oxidized, Scheme 2, upper.

Does delivery of an e^-/H^+ to the $E_2(2H)$ state of the nitrogenase cycle correspondingly create an $E_3(3H)$ state with two hydrides, one proton, and a formally oxidized core, as we have suggested, Scheme 4, or does the cofactor of the $E_3(3H)$ state contain one hydride, two sulfur-bound protons, and a reduced core? An approach like that described here in the study of Fe-nitrogenase first can be used to test the proposed generality of hydride formation in the $E_1(H)$ state of the three nitrogenase isozymes, by trapping and photolyzing the EPR-active $E_1(H)$ state of V-nitrogenase formed under low-flux conditions. The next step would then be to examine the EPR/ENDOR-active $E_3(3H)$ states of both Fe- and V-nitrogenases, trapped through use of higher-flux conditions.

Scheme 4. Cartoon of Fe 2,3,6,7 Face of FeMo-Cofactor during Accumulation of Third and Fourth $[e^-/H^+]$, with Alternative Possibilities for the Behavior of $E_3(3H)$[a]

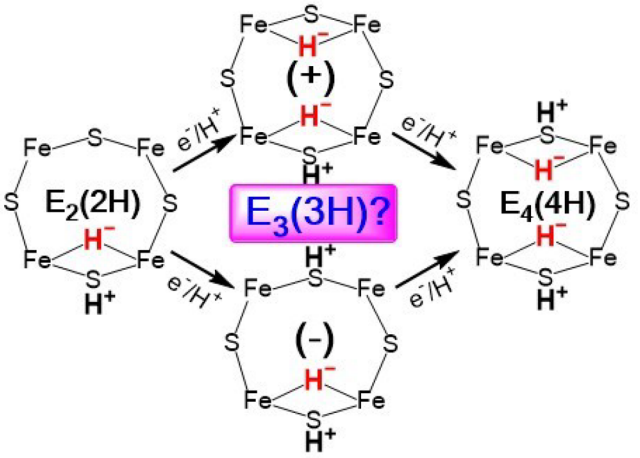

[a]We emphasize that the disposition of the hydrides, is a matter of much discussion (for example, ref 31 explicitly addresses this question).

ASSOCIATED CONTENT

Supporting Information

The Supporting Information is available free of charge at https://pubs.acs.org/doi/10.1021/acs.inorgchem.2c00180.

Three figures of EPR spectra (PDF)

AUTHOR INFORMATION

Corresponding Authors

Dennis R. Dean − *Department of Biochemistry, Virginia Polytechnic Institute and State University, Blacksburg, Virginia 24061, United States;* orcid.org/0000-0001-8960-6196; Email: deandr@vt.edu

Lance C. Seefeldt − *Department of Chemistry and Biochemistry, Utah State University, Logan, Utah 84322, United States;* orcid.org/0000-0002-6457-9504; Email: lance.seefeldt@usu.edu

Brian M. Hoffman − *Department of Chemistry, Northwestern University, Evanston, Illinois 60208, United States;* orcid.org/0000-0002-3100-0746; Email: bmh@northwestern.edu

Authors

Dmitriy A. Lukoyanov − *Department of Chemistry, Northwestern University, Evanston, Illinois 60208, United States;* orcid.org/0000-0002-4542-1648

Derek F. Harris − *Department of Chemistry and Biochemistry, Utah State University, Logan, Utah 84322, United States;* orcid.org/0000-0003-4277-2976

Zhi-Yong Yang − *Department of Chemistry and Biochemistry, Utah State University, Logan, Utah 84322, United States;* orcid.org/0000-0001-8186-9450

Ana Pérez-González − *Department of Biochemistry, Virginia Polytechnic Institute and State University, Blacksburg, Virginia 24061, United States;* orcid.org/0000-0002-7724-9985

Complete contact information is available at: https://pubs.acs.org/10.1021/acs.inorgchem.2c00180

https://doi.org/10.1021/acs.inorgchem.2c00180
Inorg. Chem. 2022, 61, 5459−5464

Notes

The authors declare no competing financial interest.

■ ACKNOWLEDGMENTS

We are grateful for support from grants from the U.S. Department of Energy, Office of Science, Basic Energy Sciences supported genetic studies, protein production, trapping of states for study, and EPR spectroscopy (DE-SC0010687, DE-SC0010834, and DE-SC0019342 to L.C.S., D.R.D., and B.M.H.) and from the National Science Foundation (MCB-1908587 to B.M.H.)

■ REFERENCES

(1) Burgess, B. K.; Lowe, D. J. Mechanism of Molybdenum Nitrogenase. *Chem. Rev.* **1996**, *96*, 2983−3012.
(2) Seefeldt, L. C.; Hoffman, B. M.; Dean, D. R. Mechanism of Mo-Dependent Nitrogenase. *Annu. Rev. Biochem.* **2009**, *78*, 701−722. PMCID: PMC2814439.
(3) Seefeldt, L. C.; Yang, Z. Y.; Lukoyanov, D. A.; Harris, D. F.; Dean, D. R.; Raugei, S.; Hoffman, B. M. Reduction of Substrates by Nitrogenases. *Chem. Rev.* **2020**, *120*, 5082−5106. PMCID: PMCPMC7703680.
(4) Harris, D. F.; Lukoyanov, D. A.; Kallas, H.; Trncik, C.; Yang, Z. Y.; Compton, P.; Kelleher, N.; Einsle, O.; Dean, D. R.; Hoffman, B. M.; Seefeldt, L. C. Mo-, V-, and Fe-Nitrogenases Use a Universal Eight-Electron Reductive-Elimination Mechanism to Achieve N_2 Reduction. *Biochemistry* **2019**, *58*, 3293−3301.
(5) Harris, D. F.; Yang, Z. Y.; Dean, D. R.; Seefeldt, L. C.; Hoffman, B. M. Kinetic Understanding of N_2 Reduction Versus H_2 Evolution at the E_4(4H) Janus State in the Three Nitrogenases. *Biochemistry* **2018**, *57*, 5706−5714. PMCID: PMCPMC6459397.
(6) Harris, D. F.; Lukoyanov, D. A.; Shaw, S.; Compton, P.; Tokmina-Lukaszewska, M.; Bothner, B.; Kelleher, N.; Dean, D. R.; Hoffman, B. M.; Seefeldt, L. C. Mechanism of N_2 Reduction Catalyzed by Fe-Nitrogenase Involves Reductive Elimination of H_2. *Biochemistry* **2018**, *57*, 701−710. PMCID: PMCPMC5837051.
(7) Lukoyanov, D.; Khadka, N.; Yang, Z. Y.; Dean, D. R.; Seefeldt, L. C.; Hoffman, B. M. Reductive Elimination of H_2 Activates Nitrogenase to Reduce the N≡N Triple Bond: Characterization of the E_4(4H) Janus Intermediate in Wild-Type Enzyme. *J. Am. Chem. Soc.* **2016**, *138*, 10674−83. PMCID: PMC5024552.
(8) Hoffman, B. M.; Lukoyanov, D.; Yang, Z. Y.; Dean, D. R.; Seefeldt, L. C. Mechanism of Nitrogen Fixation by Nitrogenase: The Next Stage. *Chem. Rev.* **2014**, *114*, 4041−62. PMCID: PMC4012840.
(9) Hoeke, V.; Tociu, L.; Case, D. A.; Seefeldt, L. C.; Raugei, S.; Hoffman, B. M. High-Resolution ENDOR Spectroscopy Combined with Quantum Chemical Calculations Reveals the Structure of Nitrogenase Janus Intermediate E_4(4H). *J. Am. Chem. Soc.* **2019**, *141*, 11984−11996. PMCID: PMCPMC6956989.
(10) Van Stappen, C.; Davydov, R.; Yang, Z. Y.; Fan, R.; Guo, Y.; Bill, E.; Seefeldt, L. C.; Hoffman, B. M.; DeBeer, S. Spectroscopic Description of the E_1 State of Mo Nitrogenase Based on Mo and Fe X-Ray Absorption and Mossbauer Studies. *Inorg. Chem.* **2019**, *58*, 12365−12376. PMCID: PMCPMC6751781.
(11) Lukoyanov, D. A.; Khadka, N.; Yang, Z. Y.; Dean, D. R.; Seefeldt, L. C.; Hoffman, B. M. Hydride Conformers of the Nitrogenase Femo-Cofactor Two-Electron Reduced State E_2(2H), Assigned Using Cryogenic Intra Electron Paramagnetic Resonance Cavity Photolysis. *Inorg. Chem.* **2018**, *57*, 6847−6852. PMCID: PMCPMC6008734.
(12) Lukoyanov, D.; Khadka, N.; Dean, D. R.; Raugei, S.; Seefeldt, L. C.; Hoffman, B. M. Photoinduced Reductive Elimination of H_2 from the Nitrogenase Dihydride (Janus) State Involves a FeMo-Cofactor-H_2 Intermediate. *Inorg. Chem.* **2017**, *56*, 2233−2240. PMCID: PMCPMC5444871.
(13) Schneider, K.; Muller, A. Iron-Only Nitrogenase: Exceptional Catalytic, Structural and Spectroscopic Features. *Catalysts for Nitrogen Fixation: Nitrogenases, Relevant Chemical Models, and Commercial Processes*; Smith, B. E., Richards, R. L., Newton, W. E., Ed.; Springer: Dordrecht, 2004; pp 281−307.
(14) Harris, D. F.; Jimenez-Vicente, E.; Yang, Z. Y.; Hoffman, B. M.; Dean, D. R.; Seefeldt, L. C. CO as a Substrate and Inhibitor of H^+ Reduction for the Mo-, V-, and Fe-Nitrogenase Isozymes. *J. Inorg. Biochem.* **2020**, *213*, 111278.
(15) Perez-Gonzalez, A.; Jimenez-Vicente, E.; Gies-Elterlein, J.; Salinero-Lanzarote, A.; Yang, Z. Y.; Einsle, O.; Seefeldt, L. C.; Dean, D. R. Specificity of NifEN and VnfEN for the Assembly of Nitrogenase Active Site Cofactors in Azotobacter Vinelandii. *mBio* **2021**, *12*, e0156821. PMCID: PMCPMC8406325.
(16) Yang, Z. Y.; Jimenez-Vicente, E.; Kallas, H.; Lukoyanov, D. A.; Yang, H.; Martin Del Campo, J. S.; Dean, D. R.; Hoffman, B. M.; Seefeldt, L. C. The Electronic Structure of FeV-Cofactor in Vanadium-Dependent Nitrogenase. *Chem. Sci.* **2021**, *12*, 6913−6922. PMCID: PMCPMC8153082.
(17) Stoll, S.; Schweiger, A. Easyspin, a Comprehensive Software Package for Spectral Simulation and Analysis in EPR. *J. Magn. Reson.* **2006**, *178*, 42−55.
(18) Hales, B. J. Alternative Nitrogenase. *Adv. Inorg. Biochem.* **1990**, *8*, 165−198.
(19) Hales, B. J.; True, A. E.; Hoffman, B. M. Detection of a New Signal in the EPR Spectrum of Vanadium Nitrogenase from *Azotobacter Vinelandii*. *J. Am. Chem. Soc.* **1989**, *111*, 8519−8520.
(20) Jasniewski, A. J.; Lee, C. C.; Ribbe, M. W.; Hu, Y. Reactivity, Mechanism, and Assembly of the Alternative Nitrogenases. *Chem. Rev.* **2020**, *120*, 5107−5157.
(21) Einsle, O.; Rees, D. C. Structural Enzymology of Nitrogenase Enzymes. *Chem. Rev.* **2020**, *120*, 4969−5004.
(22) Eady, R. R. Current Status of Structure Function Relationships of Vanadium Nitrogenase. *Coord. Chem. Rev.* **2003**, *237*, 23−30.
(23) Crabtree, R. H. *The Organometallic Chemistry of the Transition Metals*, 5th ed.; Wiley: Hoboken, NJ, 2009.
(24) Perutz, R. N.; Procacci, B. Photochemistry of Transition Metal Hydrides. *Chem. Rev.* **2016**, *116*, 8506−44.
(25) Lukoyanov, D. A.; Krzyaniak, M. D.; Dean, D. R.; Wasielewski, M. R.; Seefeldt, L. C.; Hoffman, B. M. Time-Resolved EPR Study of H_2 Reductive Elimination from the Photoexcited Nitrogenase Janus E_4(4H) Intermediate. *J. Phys. Chem. B* **2019**, *123*, 8823−8828.
(26) Lukoyanov, D.; Khadka, N.; Yang, Z. Y.; Dean, D. R.; Seefeldt, L. C.; Hoffman, B. M. Reversible Photoinduced Reductive Elimination of H_2 from the Nitrogenase Dihydride State, the E_4(4H) Janus Intermediate. *J. Am. Chem. Soc.* **2016**, *138*, 1320−7. PMCID: PMC4773049.
(27) Berberan-Santos, M. N.; Bodunov, E. N.; Valeur, B. Mathematical Functions for the Analysis of Luminescence Decays with Underlying Distributions 1. Kohlrausch Decay Function (Stretched Exponential). *Chem. Phys.* **2005**, *315*, 171−182.
(28) Lukoyanov, D.; Barney, B. M.; Dean, D. R.; Seefeldt, L. C.; Hoffman, B. M. Connecting Nitrogenase Intermediates with the Kinetic Scheme for N_2 Reduction by a Relaxation Protocol and Identification of the N_2 Binding State. *Proc. Natl. Acad. Sci. U.S.A.* **2007**, *104*, 1451−5. PMCID: PMC1785236.
(29) Raugei, S.; Seefeldt, L. C.; Hoffman, B. M. Critical Computational Analysis Illuminates the Reductive-Elimination Mechanism That Activates Nitrogenase for N_2 Reduction. *Proc. Natl. Acad. Sci. U. S. A.* **2018**, *115*, E10521. PMCID: PMC6233137.
(30) Christiansen, J.; Tittsworth, R. C.; Hales, B. J.; Cramer, S. P. Fe and Mo EXAFS of *Azotobacter Vinelandii* Nitrogenase in Partially Oxidized and Singly Reduced Forms. *J. Am. Chem. Soc.* **1995**, *117*, 10017−10024.
(31) (a) Cao, L.; Ryde, U. What Is the Structure of the E_4 Intermediate in Nitrogenase? *J. Chem. Theory Comput.* **2020**, *16*, 1936−1952. (b) Thorhallsson, A. T.; Bjornsson, R. The E_2 State of FeMoco: Hydride Formation versus Fe Reduction and a Mechanism for H_2 Evolution. *Chemistry* **2021**, *27*, 16788−16800.

https://doi.org/10.1021/acs.inorgchem.2c00180
Inorg. Chem. 2022, 61, 5459−5464